



Dissolution and powder flow characterization of solid self-emulsified drug delivery system (SEDDS)

Vikas Agarwal^a, Akhtar Siddiqui^b, Hazem Ali^b, Sami Nazzal^{b,*}

^a CIMA LABS INC., Brooklyn Park, MN, United States

^b Department of Basic Pharmaceutical Sciences, College of Pharmacy, University of Louisiana at Monroe, Monroe, LA 71209-0497, United States

ARTICLE INFO

Article history:

Received 7 May 2008

Received in revised form 10 July 2008

Accepted 27 August 2008

Available online 10 September 2008

Keywords:

Self-emulsified drug delivery systems

Solid dosage forms

Powder

Rheometry

Dissolution

Powder flow dynamics

ABSTRACT

In this study, the dynamics of powder flow upon griseofulvin-self-emulsified drug delivery system (SEDDS) addition to silica and silicates and the effect of these adsorbents on drug release were investigated. SEDDS was adsorbed at SEDDS/adsorbent ratios from 0.25:1 to 3:1 on magnesium aluminum silicate [5 and 80 μm], calcium silicate [25 μm], and silicon dioxide [3.6, 20, and 300 μm]. Powder flow was evaluated using the powder rheometer and compared to angle of repose. Release of drug from a 1:1 SEDDS/adsorbent powder was determined by dissolution using USP Type 2 apparatus. Powder rheometer profiles indicated that effect of SEDDS on the flow behavior of the adsorbents could be correlated to stepwise or continuous growing behavior as observed in wet granulation process. However, due to their porous nature, adsorbents exhibited an initial lag phase during which no change in flow was observed. Dissolution of drug from adsorbed-SEDDS was found to be dependent on pore length and nucleation at the lipid/adsorbent interface. Increase in dissolution rate was observed with an increase in surface area and was independent of the chemical nature of the adsorbents. Therefore, in order to manufacture free flowing powder containing liquid SEDDS, special attention should be given to particle size, specific surface area, type and amount of adsorbent.

© 2008 Elsevier B.V. All rights reserved.

1. Introduction

Majority of new drug candidates have poor aqueous solubility. According to an FDA survey conducted between 1995 and 2001, only 9% of the new drug molecules belonged to BCS Class I category (Brown, 2005). By adopting different strategies, such as complexation with cyclodextrin, solid dispersion, and self-emulsifying drug delivery system, solubility and thereby bioavailability of drugs can be improved (Nazzal et al., 2002a).

Griseofulvin, a systemic antifungal drug, was selected in this study as a model drug, which displays poor solubility and low bioavailability when administered orally in the form of tablet, capsule, and suspension (Vyas et al., 1992). These problems laid ground for the development and optimization of a lipid based formulation of griseofulvin in this study. In practice, lipid formulations are a diverse group of formulations, which result from the blending of up to five classes of excipients such as pure triglyceride oils, mixed glycerides, lipophilic surfactants, hydrophilic surfactants and water-soluble co-solvents (Pouton, 2000). Of the different lipid formulations, much attention has been paid to the

self-emulsifying drug delivery system or self-emulsified drug delivery system (SEDDS), which were demonstrated to augment oral bioavailability of many drugs such as halofantrine (Khoo et al., 1998), Ontazolest (Hauss et al., 1998), Cyclosporine (Klauser et al., 1997) and Progesterone (MacGregor and Embleton, 1997).

SEDDS are generally encapsulated either in hard or soft gelatin capsules. Lipid formulations however may interact with the capsule resulting in either brittleness or softness of the shell (Chang et al., 1998; Nazzal and Wang, 2001; Mei et al., 2006). To address this limitation, liquid lipid formulations could be transformed into free flowing powder by loading the formulation on a suitable solid carrier (Nazzal et al., 2002b; Pather et al., 2001, 2004). Liquid lipid loading onto solid carriers combines the features of a lipid based drug delivery system and solid dosage form (Cannon, 2005). SEDDS loaded powder however should have acceptable flow properties to facilitate capsule or tablet manufacturing in order to pass compendial limit for content uniformity and weight variation. Various methods were used to incorporate lipids into solid matrices, which were summarized in recently published reviews (Cannon, 2005; Jannin and Chambin, 2005). In several studies, "solid solutions" and "liquisolds" have been prepared by converting drug solution in nonvolatile solvent into an apparently dry, nonadherent powder using silica of large surface area as an adsorbent (Yang and Glemza, 1979; Liao and Jarowski, 1984; Spireas et al., 1992, 1998;

* Corresponding author. Tel.: +1 318 342 1726; fax: +1 318 342 1737.
E-mail address: nazzal@ulm.edu (S. Nazzal).

Spireas and Sadu, 1998). On similar line, DeHaan and Poel-Janssen (2001) and Pather et al. (2001) developed solid dosage forms based on microemulsion adsorption onto colloidal silicon dioxide. The limitation of these studies was their reliance on angle of repose as the measure of powder flow without providing a mechanistic explanation of the effect of the adsorbed lipids on powder flow. Furthermore, they did not address the mechanisms involved in drug release from lipids adsorbed on silica adsorbents. Only recently, it was however reported that hydrogen bonding and Oswald ripening play a critical role in drug release from these systems (Gupta et al., 2002).

Angle of repose is one of several methods, which potentially could be used to characterize and measure the flow properties of the powdered SEDDS formulations. For example, chapter 1174 “powder flow” of the USP identified four conventional methods for characterizing powder flow; angle of repose, compressibility index and Hausner ratio, flow through an orifice, and shear shell methods. Although each of these methods describes certain aspect of powder behavior, it certainly has limitations, such as segregation, consolidation and aeration during cone formations; dependency on instrument dimensions, and labor and time intensiveness (USP30/NF29). Mixture torque rheometer has also been used to measure flow properties of powders and is widely employed in the characterization of the wet granulation process (Hariharan and Mehdizadeh, 2002; Chatlapalli and Bhagwan, 1998; Luukkonen et al., 2001). In this method, torque or the resistance to the movement of the impeller is measured, whereby powder having greater permeability or non-cohesiveness show less resistance in comparison to cohesive or less permeable powders. Similarly, powder rheometer has recently been introduced as an alternative method to characterize flow properties of both dry and wet powder masses (Luukkonen et al., 2001; Podczek and Newton, 2000; Podczek, 1999; Freeman, 2004).

In addition to its versatile applications, this instrument has the advantage of generating real-time torque data and producing reproducible results by incorporating conditioning cycles in the method, which eliminate filling stresses and differences in filling technique by slicing and aerating the powder bed through upward and downward movement of probe.

Previously, we have shown that lipids can act as non-aqueous granulating aids similar to aqueous granulating aids (Nazzal et al., 2002a,b). Powder rheometry could be used as an instrumental method to further improve our understanding of the impact of lipids on powder flow and an alternative method to characterize the granulation process. Therefore, the primary objective of this study was to investigate the dynamics of powder flow upon gradual addition of griseofulvin-SEDDS formulation to silica and silicate adsorbents using a powder rheometer. The secondary objective was to investigate the effect upon adsorption of the type of silica and silicate adsorbents at fixed ratio of SEDDS to various types of adsorbents on the dissolution of the powdered formulation and the release of griseofulvin as a function of adsorbent characteristics.

2. Materials and methods

2.1. Materials

Micronized griseofulvin, USP (mean particle size 12 μm) was obtained from Hawkins, Inc., Pharmaceutical group (Minneapolis, MN). Captex 355 (triglycerides of caprylic/capric acid) was supplied by ABITEC Corporation (Janesville, WI). Tween 80 (polyoxyethylene sorbitan mono oleate) was provided by Uniqema (New Castle, DE). Labrasol (C₈/C₁₀ polyglycolized glycerides from coconut oil) was provided by Gattefosse (Saint-Priest Cedex, France). Calcium silicates (Hubersorb 5121[®]) and synthetic amorphous silica

(ZeoPharm 5170[®], Rxcipients GL100[®], and Rxcipients GL200[®]) were obtained from Huber Engineering Material (Atlanta, GA). Magnesium aluminum silicates (Neusilin US2[®] and Neusilin UFL2[®]) were provided by Fuji Health Science, Inc. (Mount Laurel, NJ). Hard gelatin capsules (size 000) were provided by Eli Lilly & Company (Indianapolis, IN). Acetonitrile HPLC grade was purchased from EMD Chemical Inc. (Gibbstown, NJ). Tetrahydrofuran HPLC grade was purchased from J.T. Baker Chemical Co. (Phillipsburg, NJ). Water used was freshly prepared by a combination of demineralization and reverse osmosis using a NANO pure system (Barnstead, Dubuque, IA). All items were used as supplied without further modification.

2.2. Preparation of griseofulvin-SEDDS formulation (G-SEDDS)

Tween 80 (45%), Labrasol (30%), Captex 355 (5%), and griseofulvin (1%) were accurately weighed and transferred into a borosilicate glass vial. Using magnetic stirrer, the ingredients were mixed for 10 min at 60–65 °C until a yellowish transparent formulation was attained. Griseofulvin lipid formulations were then allowed to cool to room temperature before they were used in subsequent studies. To characterize the resultant blend, the emulsification of the lipid formulation in water was visually examined as described by Kommuru et al. (2001) and the droplet size of the microemulsion was estimated by dynamic light scattering using Nicomp[®] 380 particle size analyzer (PCC Nicomp, Santa Barbara, CA). For simplicity, the liquid griseofulvin lipid formulation will be termed G-SEDDS in subsequent discussion.

2.3. Adsorption of G-SEDDS on silica and silicates

Silica derivatives, calcium silicate (25 μm), magnesium aluminum silicate (5 and 80 μm), and silicon dioxide (3.6, 20, and 300 μm) were used as the solid adsorbents to load G-SEDDS. The physical characteristic of each adsorbent/carrier is summarized in Table 1. The lipid formulation was added in increments and blended with the adsorbent at the following fixed G-SEDDS to adsorbent ratios by weight: 0.25:1, 0.5:1, 0.75:1, 1:1, 1.25:1, 1.5:1, 2:1, 2.25:1, 2.5:1, 3:1, 3.25:1. Briefly, a constant aliquot of G-SEDDS was initially added to and mixed with the adsorbent in a mortar. Batch size of each blend varied with the density of the adsorbent (Table 1), and was determined based on the quantity required to occupy approximately 120 cm³ of the total volume of the cylindrical glass vessel of the powder rheometer. The flow behavior of the adsorbed blend was then analyzed as described in the subsequent section. Addition of G-SEDDS to the adsorbent however was discontinued once a non-flowing cohesive mass is formed.

2.4. Powder rheometry

TA.XTPlus Texture Analyzer fitted with a powder flow analyzer (Texture Technologies Corp., Scarsdale, NY/Stable Micro Systems, Godalming, Surrey, UK) was used for characterization of powder flow. At the beginning of each experiment, the instrument was calibrated for force and distance. After calibration of the powder rheometer, calcium silicate (25 μm), magnesium aluminum silicate (5 and 80 μm) and silicon dioxide (3.6, 20, and 300 μm) adsorbents were analyzed individually prior to G-SEDDS addition, thereby acting as control. For analysis, a cylindrical glass vessel with a capacity of 200 ml was initially placed on the platform of the instrument. Then, sufficient amount of the adsorbent was poured into the cylindrical vessel to create a powder bed that is 60 mm high and occupies 120 cm³ of the total volume of the vessel. After analysis, the adsorbent was removed from the vessel and placed in a mortar. G-SEDDS was then adsorbed to this volume of adsorbent after which the

Table 1
Physical characteristics of adsorbents used in this study.

Chemical nature	Calcium silicate	Magnesium aluminum silicate	Magnesium aluminum silicate	Silicon dioxide	Silicon dioxide	Silicon dioxide
Trade name	Hubersorb 5121 [®]	Neusilin US2 [®]	Neusilin UFL2 [®]	ZeoPharm 5170 [®]	Rxcipients GL100 [®]	Rxcipients GL200 [®]
Physical form	Spray dried Powder	Powder	Spherical fine granule	"Pelletized" white powder	Dried white powder	Dried white powder
Mean particle size (μm)	25	80	5	300	3.6	20
Oil adsorbing capacity (ml/100 g)	90	300	310	168	215	220
Reported maximum adsorption ratio ^a	0.9:1	3:1	3:1:1	1.68:1	2.15:1	2.2:1
Observed maximum adsorption ratio ^b	1:1	3:1	2.75:1	1.75:1	2:1	2.75:1
Specific surface area (m^2/g) BET	50	300	300	165	150–200	160
Bulk density (lb/ft^3)	25	9–18 (ml/g)	4–6 (ml/g)	17	4–8	5–9
5% slurry pH	9	7.4	7.4	6–7	6.5–7.5	6.5–7.5

^a Relative value representing the ratio of oil adsorption capacity of 1 g powder.

^b Relative value representing the ratio of G-SEDDS adsorption capacity of 1 g powder, which is the % G-SEDDS loading at the end of the capillary stage and the % G-SEDDS loading prior to the formation of a dispersion state in a stepwise and continuous growing behaviors, respectively.

blend was placed in the cylindrical vessel for flow analysis. This step was repeated for each G-SEDDS to adsorbent ratio ranging from 0.25:1 to 3.25:1 in stepwise increments of 0.25. Flow analysis was performed on the blends irrespective of their weight or volume. During analysis, each powder was subjected to one conditioning and three test cycles. The conditioning cycle was essential to eliminate filling stresses and/or differences between the blends arising from differences in the filling technique. Conditioning was performed by slicing and aerating the powder bed through upward and downward movement of probe in a clockwise direction. Each test cycle was performed in compression mode in which the probe moves downward (clockwise) in a helical path at an angle of 45° and at a speed of 10 mm/s followed by an upward (anticlockwise) helical movement at angle of 175° with a speed of 50 mm/s. Data collected from the effective powder zone in the cylindrical column was used for analysis and interpretation. Effective powder zone was chosen as the middle two third of the powder bed. In this zone, the probe remains completely immersed in the powder and is devoid of back pressure observed at the bottom of the vessel (Navaneethan et al., 2005). The resistance experienced by the probe as a function of distance was automatically plotted and recorded. A representative force displacement curve generated by the instrument is given in Fig. 1. The area under the force displacement curves was measured as the work done by the blade in passing through the powder bed.

2.5. Measurement of angle of repose

Angle of repose for the adsorbents alone and the adsorbents blended with G-SEDDS were determined by Carr's method (1965). Briefly, a glass funnel was secured with its tip positioned at a fixed height (H) above a wax paper placed on a horizontal surface. The sample was poured through the funnel until the apex of the conical pile reached the tip of the funnel. The angle of repose was calculated using the formula $\tan \alpha = H/R$, where α is the angle of repose and R is the radius of the conical pile.

2.6. In vitro dissolution studies

In vitro dissolution studies were performed on micronized griseofulvin pre-blended with lactose as a diluent, liquid G-SEDDS, and G-SEDDS adsorbed on each carrier at 1:1 ratio. Dissolution studies were also performed on G-SEDDS adsorbed on silicon dioxide ($3.6 \mu\text{m}$ [GL100[®]]) at ratios of 1.5:1, 1:1, and 0.5:1. Briefly, 500 mg of liquid G-SEDDS or 1 g of powdered G-SEDDS (1:1), each equivalent to 5 mg of griseofulvin was filled into hard gelatin capsules of size 000. In the case of silicon dioxide ($3.6 \mu\text{m}$ [GL100[®]]), 833 mg of the 1.5:1 ratio, 1 g of the 1:1 ratio, and 1.5 g of the 0.5:1 ratio were used, each equivalent to 5 mg of griseofulvin. Dissolution studies were performed in 100 ml of water as the dissolution medium using USP

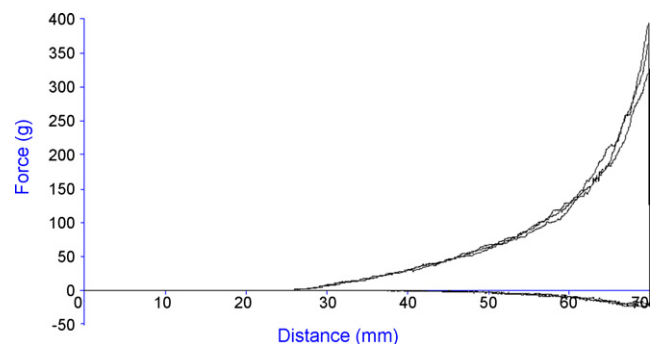


Fig. 1. A representative force–displacement curve generated by the powder rheometer for one of the powder blends showing the three test cycles.

Type 2 apparatus (VK7000) fitted with 200 ml mini-conversion kits (Varian Inc. Cary, NC). Griseofulvin is a non-ionizable molecule, and therefore the pH of the medium is not expected to have an effect on dissolution. Furthermore, no surfactants were added to the medium to avoid sink conditions. Thereby data generated from the dissolution study are a direct measure of the emulsification efficiency of the SEDDS formulation. Paddle speed and bath temperature were set to 75 rpm and 37 °C, respectively. Samples (5 ml) were collected at different time intervals and analyzed by HPLC. Dissolution experiments were performed in triplicates unless otherwise specified.

2.7. HPLC analysis

The amount of griseofulvin released in dissolution medium was quantified at ambient temperature by reverse phase HPLC using Luna 5 μ CN 100A, 250 mm \times 4.6 mm column (Phenomenex, Torrance, CA). An SP Thermo separation HPLC instrument (Thermo Electron, San Jose, CA) was used, which consisted of P-2000 pump, AS-1000 autosampler, and UV-3000 detector set at a wavelength of 290 nm. Before analysis, samples were diluted with the mobile phase at a ratio of 1:1. The mobile phase consisted of water, acetonitrile and tetrahydrofuran (6:3.5:0.5) and was pumped at a flow rate of 1 ml/min. The chromatographic data was managed by ChromQuest 4.2 software (Thermo Electron, San Jose, CA).

3. Results and discussion

3.1. Powder flow characterization

The flow behavior exhibited by the powder blends was determined on the basis of force or torque exerted by the probe in traversing powder bed as a function of amount of G-SEDDS added. Depending upon the nature of powder, the probe will exert different levels of torque on powder bed. In the case of non-cohesive and free flowing powders, the blade exerts less force or torque as the particles freely cascade above and around the blade. In cohesive powder, particles are attached by liquid bridges or hydrophobic bonds. The additional force required for the blade to sever these interactions results in higher torque values. Nonetheless, torque applied by the blade is decreased when the powder enters into a dispersion state with the addition of excess amount of liquid.

Our experiments indicated that the addition of a SEDDS formulation to a solid adsorbent exhibited similar flow behavior as the addition of granulating fluid to a powder during the wet granulation process. With the addition of a granulating fluid, the powder undergoes gradual transformation into four states: pendular, funicular, capillary and dispersion states (Goldszal and Bousquet, 2001). The systematic transition of powders from one stage to another is referred to as stepwise growing behavior (Goldszal and Bousquet, 2001). Another group of powders exhibits no critical agglomerate size; rather they form a single agglomerate or paste of all the available particles (equivalent of pendular state). Such transition of powder directly into an agglomerated state is referred to as continuous growing behavior.

The rheometric plots for adsorbents with average particle size $\leq 20 \mu\text{m}$ are given in Fig. 2. Initially, magnesium aluminum silicate (5 μm), and silicon dioxide (3.6 and 20 μm) adsorbents exhibited a reduction in torque after the addition of G-SEDDS to the adsorbents. At a 0.25:1 ratio of G-SEDDS to magnesium aluminum silicate (5 μm), and silicon dioxide (3.6 and 20 μm), work done relative to G-SEDDS-free powder by probe in traversing the powder beds decreased from 9.9, 9.6, 11.9 g-force mm to 7.6, 7.5, and 7.4 g-force mm, respectively (Fig. 2). The observed reduction in torque after the initial addition of G-SEDDS is due to a ball-bearing effect, which reduced the friction between the particles. The work done

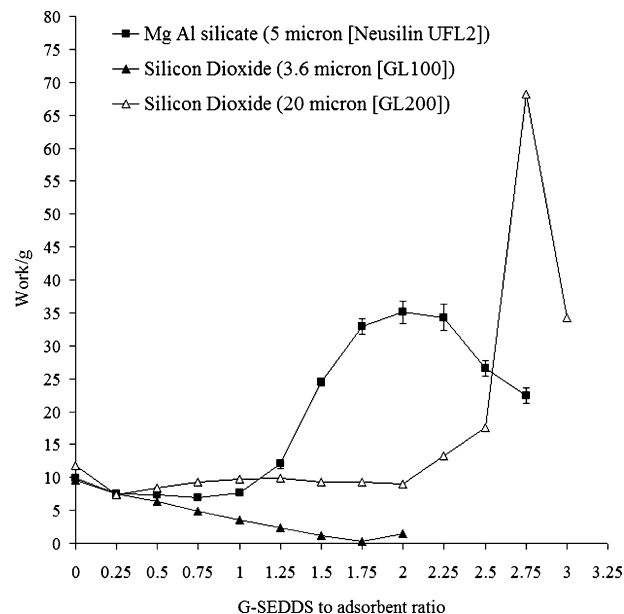


Fig. 2. Rheometric plots showing the work done per gram of the powder blend as a function of G-SEDDS loading on silicon dioxide (3.6 and 20 μm), and magnesium aluminum silicate (5 μm).

on the powder bed however did not change upon successive liquid addition until G-SEDDS to magnesium aluminum silicate (5 μm), and silicon dioxide (3.6 and 20 μm) ratios reached 1:1, 1.75:1, and 2:1, respectively. No change in flow was observed during this period due to the adsorption capacity of the adsorbents and retention of G-SEDDS in their intraparticle pores. On visual inspection, all powders were dry and free flowing at this point.

As the G-SEDDS to magnesium aluminum silicate (5 μm) ratio increased to 1.75:1, the work done relative to G-SEDDS-free powder increased to 32.9 g-force mm. Increase in torque suggests that G-SEDDS formed liquid bridges between the particles. The formation of liquid bridges, which is being considered similar to the pendular state in wet granulation, would increase cohesiveness of the powder and result in an increase in work done by the probe. Further, G-SEDDS addition to magnesium aluminum silicate (5 μm) to a ratio of 2.25:1, resulted in a plateau and no net increase in torque (Fig. 2), which is considered similar to the funicular state in wet granulation. Thereafter, magnesium aluminum silicate (5 μm) underwent a capillary state as the G-SEDDS to adsorbent ratio increased above 2.25:1 (Fig. 2). This stage was characterized by an initial reduction in work done followed by an increase in torque and loss of flowability due to simultaneous filling of inter-particle spaces as well as formation of bridges between agglomerates. However, the increase in torque could not be measured for magnesium aluminum silicate (5 μm) because it exceeded the capacity of the load cell of the texture analyzer.

Similarly, as the G-SEDDS to silicon dioxide (20 μm) ratio increased to 2.5:1, the work done relative to G-SEDDS-free powder increased to 17.6 g-force mm. Silicon dioxide (20 μm), however, did not exhibit a funicular state; rather a sharp increase in work done was observed as the ratio of G-SEDDS to silicon dioxide (20 μm) increased from 2.5:1 to 2.75:1. At this ratio, the difference in work done with respect to G-SEDDS-free powder was 60 g-force mm. This increase in work done resembles the capillary state in wet granulation whereby G-SEDDS filled the interparticle voids and formed bridges between the agglomerates. Further addition of G-SEDDS to silicon dioxide (20 μm) beyond 2.75:1 ratio resulted in the formation of a solid/liquid dispersion state characterized by reduction in

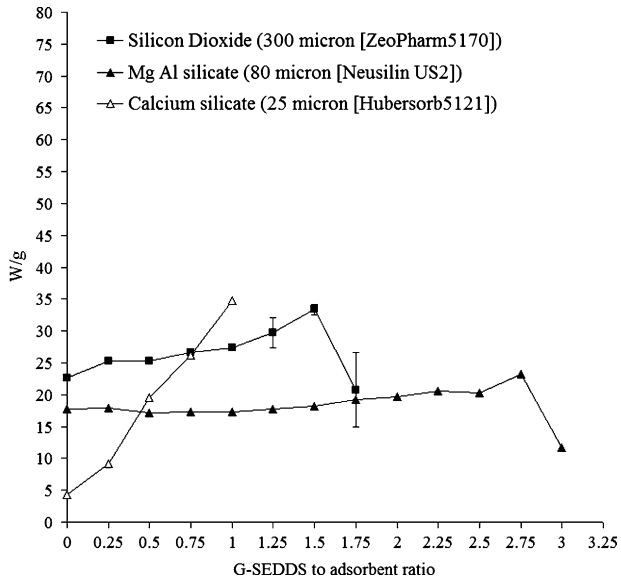


Fig. 3. Rheometric plots showing the work done per gram of the powder blend as a function of G-SEDSS loading on silicon dioxide (300 μm), magnesium aluminum silicate (80 μm), and calcium silicate (25 μm).

torque. At this stage the powder bed appeared oily and turned into a translucent greasy mass.

In the case of silicon dioxide (3.6 μm), work done on the powder bed increased from 0.23 g-force mm at 1.75:1 ratio to 1.5 g-force mm at 2:1 ratio. As with silicon dioxide (20 μm), silicon dioxide (3.6 μm) did not exhibit a funicular state. Further addition of G-SEDSS to silicon dioxide (3.6 μm) beyond 2:1 ratio formed solid agglomerates whose flow resistance exceeded the torque limit of the instrument. Therefore, addition of G-SEDSS to silicon dioxide (3.6 μm) was terminated and no additional experiments were performed.

The rheometric plots for adsorbent with average particle size $>20 \mu\text{m}$ are given in Fig. 3. Magnesium aluminum silicate (80 μm) and silicon dioxide (300 μm) exhibited continuous growing behavior rather than stepwise growing behavior. They demonstrated no decrease in torque at a ratio of 0.25:1. They were dry, non-sticky, and free flowing until G-SEDSS to magnesium aluminum silicate (80 μm) and silicon dioxide (300 μm) ratios of 2.5:1, 1:1, respectively. Higher ratio observed with magnesium aluminum silicate (80 μm) is due to its higher specific surface area and oil adsorbing capacity than silicon dioxide (300 μm) (Table 1). Further addition of G-SEDSS beyond these ratios resulted in an increase in work done because of sudden formation of paste or single agglomerate, which corresponds to a pendular state in stepwise growing behavior. The observed reduction in torque at G-SEDSS to magnesium aluminum silicate (80 μm) and silicon dioxide (300 μm) ratios of 3:1 and 1.75:1, respectively, is due to the excess liquid and formation of wet powdery mass.

In comparison to other adsorbents, calcium silicate (25 μm [Hubersorb 5121[®]]) has the least oil adsorbing capacity and specific surface area (Table 1). Poor adsorption is reflected in its rheometric profile (Fig. 3), which shows an immediate and steady increase in torque with successive addition of G-SEDSS. Increase in torque is an indication of a pendular state and the formation of liquid bridges between the particles. At ratio greater than 1:1, the presence of excess liquid resulted in the formation of a wet solid mass that required torque values that exceeded the limits of the load cell.

Based on the mechanistic explanation of wet granulation, magnesium aluminum silicate (5 μm), and silicon dioxide (3.6 and 20 μm), whose mean particle size lie between 1 and 20 μm , showed

resemblance to stepwise growing behavior whereas magnesium aluminum silicate (80 μm), silicon dioxide (300 μm) and calcium silicate (25 μm) which have mean particle size $>20 \mu\text{m}$ exhibited similarity to continuous growing behavior. This information is particularly valuable to set optimal quantity of SEDDS addition in batch manufacturing. For powder exhibiting stepwise growing behavior, funicular (plateau) state was shown to be the critical point for obtaining free flowing powder with minimum instability and better control of the process (Goldszal and Bousquet, 2001). However, the funicular state was not distinctly observed in continuous growing behavior because of sudden shift in states from free flowing to paste during SEDDS addition. Therefore rheometry data for powders exhibiting continuous growing behavior cannot be readily used to deduce the optimal SEDDS to powder ratio.

Based on the powder rheometry data, the maximum ratio of G-SEDSS to calcium silicate (25 μm), magnesium aluminum silicate (5 and 80 μm) and silicon dioxide (3.6, 20, and 300 μm) at which free flowing powders were obtained are 1:1, 2.25:1, 2.5:1, 2:1, 2.5:1, 1:1, respectively. These observed values are less than the maximum reported adsorption capacity of the powders (Table 1), further demonstrating the usefulness of the powder rheometer in determining the end point for SEDDS addition.

To further illustrate the valuable information obtained from the powder rheometry data, angle of repose measurements were performed on the solid adsorbents and the various G-SEDSS blends that were used in the powder rheometry studies. Historically, angle of repose has been used to measure the properties of pharmaceutical materials, primarily because of its ease of determination (Amidon, 1995). However, poor correlation between angle of repose and other measures of flow has been reported (Thalberg et al., 2004). Therefore, angle of repose has not been considered reliable predictor of powder flow (Amidon, 1995). This is illustrated in Fig. 4, which shows the angle of repose of the powder blends at various G-SEDSS to adsorbent ratios. As seen in the figure, no correlation could be observed between the physicochemical nature of the adsorbents at various G-SEDSS ratios and the angle of repose. Angle of repose remained either constant or increased with subsequent additions of G-SEDSS. At high G-SEDSS to adsorbent ratios, the angles obtained were similar at a level just above 40°. This might

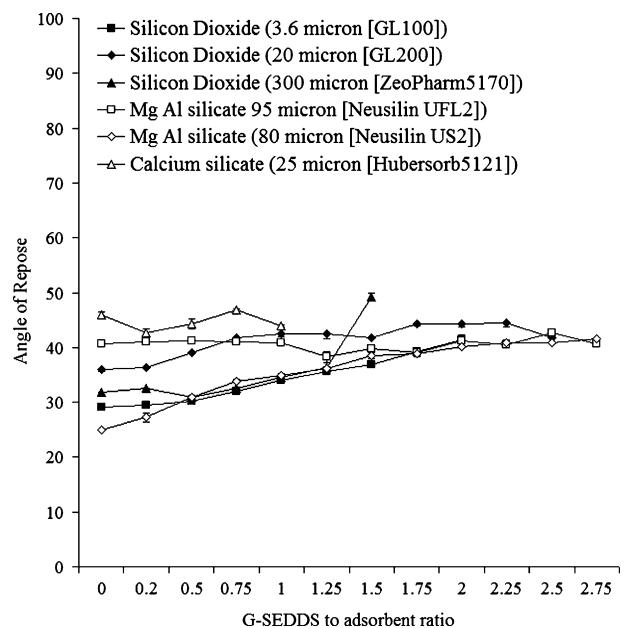


Fig. 4. Angle of repose measured for the adsorbents alone and the adsorbents blended with G-SEDSS.

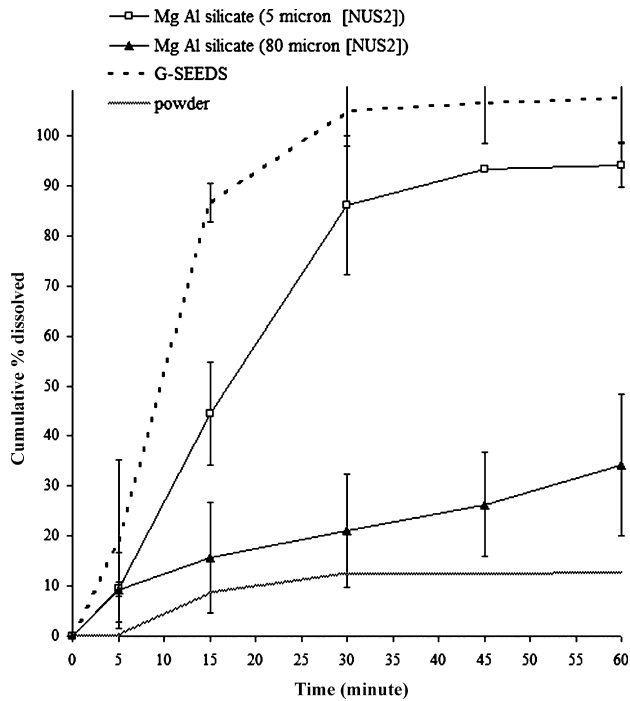


Fig. 5. Dissolution profiles of liquid G-SEDDS, micronized griseofulvin powder, and G-SEDDS adsorbed on magnesium aluminum silicate (5 and 80 μm) at a 1:1 ratio.

be due to the difficulty in measuring angle of repose for cohesive powders (Thalberg et al., 2004). While powder rheometry accurately predicted an increase in cohesiveness of the powders with the addition of G-SEDDS, angle of repose study failed to delineate the different phases that adsorbent undergo with the addition of G-SEDDS.

3.2. Dissolution study

By definition, SEDDS are isotropic mixtures of oil, surfactant, co-surfactant, and drug, which form fine o/w emulsions when introduced into an aqueous phase under gentle agitation (Nazzal et al., 2002a; Craig et al., 1993). The optimized composition of the G-SEDDS formulation described in Section 2.2 above was based on preliminary solubility and formulation optimization data (data not shown). To verify that the formulation falls within the definition of self-emulsified drug delivery systems, the emulsification of this formulation was visually examined and the droplet size of the resultant dispersion was measured. Upon contact with the dissolution medium, the liquid G-SEDDS spontaneously dispersed into a transparent solution with an average droplet size of 7.25 nm, which is approximately within the size-range observed in microemulsion systems (Greiner and Evans, 1990). The dissolution profile of the liquid G-SEDDS is given in Fig. 5. As depicted in the figure, the average cumulative percent of griseofulvin released from the liquid G-SEDDS in 15 min was 86.5% whereas the cumulative percent of the micronized griseofulvin powder dissolved in 15 min was 8.6%.

The dissolution profiles of the G-SEDDS adsorbed on silica and silicates are given in Figs. 5–7. As depicted in the figures, the release of griseofulvin from the adsorbents lies intermediate between the maximum release by liquid G-SEDDS and minimum release by the micronized griseofulvin powder. The cumulative percent of griseofulvin released from liquid G-SEDDS, magnesium aluminum silicate (5 and 80 μm), calcium silicate (25 μm), silicon dioxide (3.6, 20, and 300 μm) and micronized griseofulvin powder after 60 min was approximately 100, 94.0, 34.2, 26.0, 42.6, 44.0, 27.0, and 12.8%,

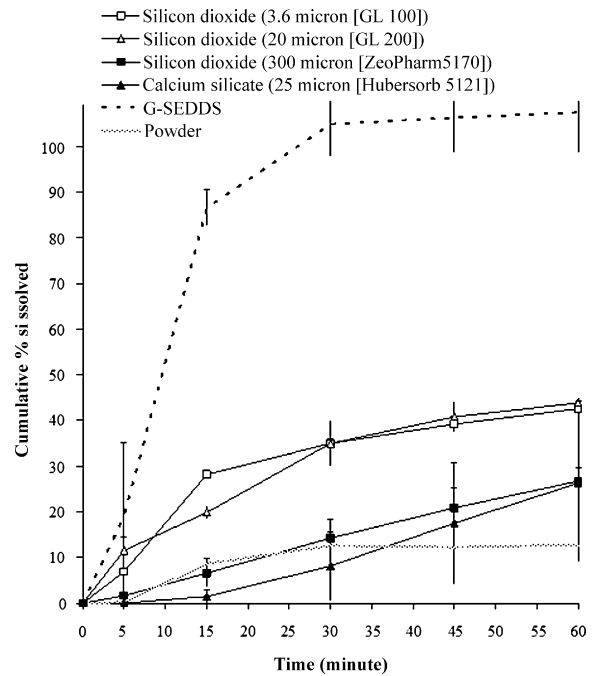


Fig. 6. Dissolution profiles of liquid G-SEDDS, micronized griseofulvin powder, and G-SEDDS adsorbed on silicon dioxide (3.6, 20, and 300 μm) and calcium silicate (25 μm) at a 1:1 ratio.

respectively. As depicted in Figs. 2 and 3 and discussed in Section 2.3 above, at G-SEDDS to adsorbent ratio of 1:1, all powder blends, with the exception of calcium silicate (25 μm [Hubersorb 5121[®]]), existed in free flowing form where liquid G-SEDDS is retained within the intraparticulate pores of the solid carrier. At this ratio, however, calcium silicate (25 μm [Hubersorb 5121[®]]) existed in agglomerated form with the liquid G-SEDDS adsorbed on the external surface of the adsorbent.

Since the depth and density of pores is a function of the specific surface area and particle size of the adsorbents, we hypothesized

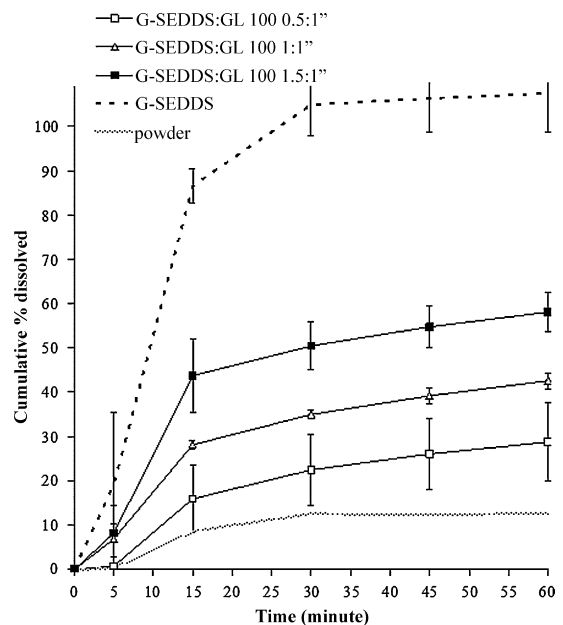


Fig. 7. Dissolution profiles of liquid G-SEDDS, micronized griseofulvin powder, and G-SEDDS adsorbed on silicon dioxide (3.6 μm) at 0.5:1, 1:1, and 1.5:1 ratios.

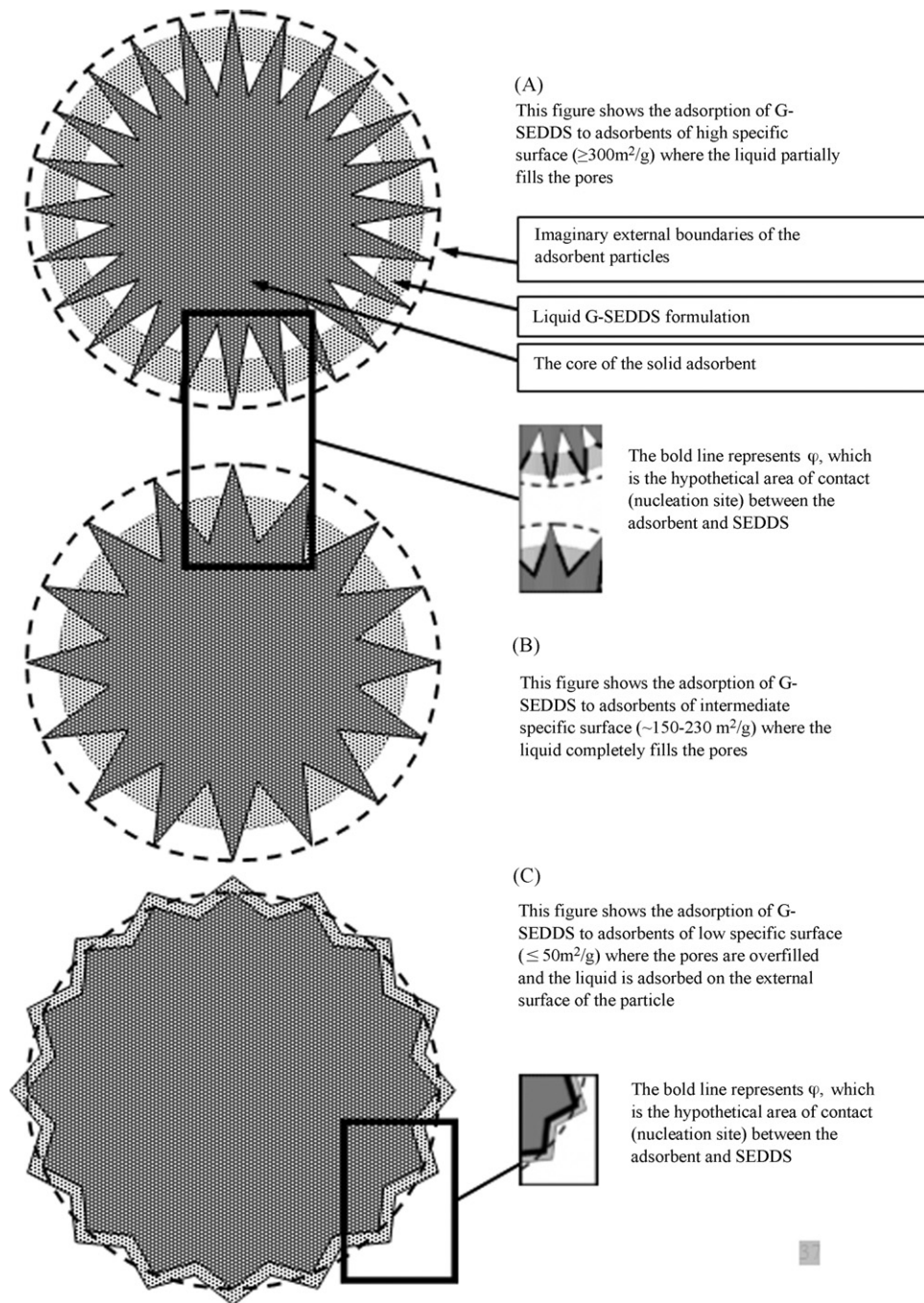


Fig. 8. A schematic diagram showing the different possibilities for the adsorption of SEDDS on adsorbents of varying surface area.

that at G-SEDDS to adsorbent ratio of 1:1 the lipid formulation would be retained within the pores in one of several forms given in Fig. 8. These forms explain the observed dissolution data outlined in subsequent discussion. A lipid formulation could either partially (Fig. 8A) or completely fill (Fig. 8B) intraparticle pores of the adsorbent; or, in the case of adsorbent with low specific surface area adsorbed as thin films on the surface of adsorbents (Fig. 8C). The type of retention determines the total area of contact between the formulation and either the surface of the adsorbent or the walls of its pores, both of which are reflected by the symbol φ in Fig. 8. These areas (φ) may act as nucleation sites for griseofulvin, which is dissolved in the SEDDS formulation. A greater area of contact (φ) leads to a greater nucleation rate and subsequent precipitation of

griseofulvin. The impact of contact area (φ) on nucleation is based on the fact that the surface properties of silica significantly affect drug affinity to its surface. For example, the presence of silanol groups on the surface of silica and silicate make it a potential proton donor as well as an acceptor (Gupta et al., 2002). The induction of low energy bond like van der Waal and London forces between the surface of the adsorbent and hydrophobic drug molecules, such as griseofulvin in the SEDDS formulation, may become significant. Such forces are expected to induce drug aggregation or coalescence, particularly with hydrophobic drugs whose concentration in SEDDS is approaching saturation solubility (Salonen et al., 2005). Griseofulvin, a high-energy crystal type compound, is therefore expected to exhibit high affinity to the hydrophobic surface of

the silica based adsorbents, which was previously reported by Salonen (Hodes, 2002). This affinity would be manifested by the preferential diffusion of griseofulvin from the SEDDS to the surface of the adsorbent (φ). Subsequent nucleation will result in the precipitation of griseofulvin due to its poor solubility in the dissolution medium. The highest nucleation rate is expected in adsorbents with low specific surface ($\leq 50 \text{ m}^2/\text{g}$, Fig. 8C). Because of the limited area available for adsorption, G-SEDDS forms thin film on the surface of the adsorbent thereby maximizing the total area of contact (φ). On the other hand, at low levels of SEDDS loading, lowest nucleation rate is expected with porous adsorbents of high specific surface ($\geq 300 \text{ m}^2/\text{g}$, Fig. 8A) in which microporosities act as capillary channels whereby G-SEDDS are entrained as droplets rather than adsorbed to the surface of the adsorbent. G-SEDDS entrainment minimizes the area of contact between the adsorbent and SEDDS. The impact of contact area (φ) on griseofulvin release is demonstrated in the subsequent discussion.

The cumulative percent of griseofulvin released from 5 and 80 μm magnesium aluminum silicate adsorbents was 44.5 and 15.7% after 15 min and 86.1 and 21.1% after 30 min, respectively. Magnesium aluminum silicate (5 μm) has spherical granules with mean particle size distribution between 2 and 8 μm . Taking its size into consideration, magnesium aluminum silicate (5 μm [Neusilin UFL2[®]]) exhibits high oil adsorbing capacity and specific surface area, which were reported to be 310 and 300 m^2/g , respectively. As discussed above, the entrainment of G-SEDDS in the porous magnesium aluminum silicate (5 μm), which is depicted in Fig. 8A, limits drug exposure to the surface of the adsorbent and explains the overall high extent of griseofulvin release (Fig. 5). The cumulative percent of griseofulvin released from magnesium aluminum silicate (5 μm) at 15, 30, 45, and 60 min, however, was significantly lower ($p < 0.05$) than the release data obtained for G-SEDDS in the absence of adsorbent. This is due to precipitation of griseofulvin at the contact interface (φ) between G-SEDDS and the adsorbent.

Magnesium aluminum silicate (80 μm [Neusilin US2[®]]) has larger particle size and similar specific surface area (300 μm) as magnesium aluminum silicate (5 μm). This suggests the presence of larger number of long and narrow intraparticle pores, which contribute to the creation of surface area equivalent to those observed with magnesium aluminum silicate (5 μm [Neusilin UFL2[®]]). The lower percentage drug release in 15 min in comparison to magnesium aluminum silicate (5 μm) could be attributed to the entrapment of the formulation in the tortuous pores. The relationship between pore length and rate of leaching is expressed by the Poiseuille's equation. According to this model, an increase in pore length is expected to diminish formulation release. Similar observation was reported for the release and dissolution of loratadine SEDDS from porous polystyrene beads (Patil and Paradkar, 2006). Gradual release of griseofulvin in subsequent time points is due to gradual access of water to the G-SEDDS present in these pores.

The silicon dioxide adsorbents (3.6, 20, and 300 μm) have mean specific surface area of 150–200, 160, and 165 m^2/gm , respectively. The release profiles of griseofulvin from silicon dioxide (3.6 and 20 μm) are given in Fig. 6. Dissolution data indicate that there is no significant difference ($p > 0.05$) in the cumulative percent of griseofulvin released from both adsorbents after 30 min. This implies that size differences between the two adsorbents did not influence drug release. It is probable that at this size range (1–20 μm), the physical difference in term of pore size and length are not substantially different to warrant significant differences in drug release.

Although the particle size of magnesium aluminum silicate (5 μm) and silicon dioxide (3.6 μm) falls in the same range, the average cumulative percentage of griseofulvin released from both adsorbents after 15 min were 44.5 and 28.1%, respectively. The lower extent of griseofulvin release observed with silicon dioxide

(3.6 μm [GL100[®]]) is due to its lower specific surface area. Therefore, with silicon dioxide (3.6 μm), a greater portion of the G-SEDDS is in direct contact with the adsorbent (Fig. 8B), which leads to precipitation and subsequently lower dissolution rates.

The cumulative percent of drug released from silicon dioxide (300 μm [GL200[®]]) was 6.58% in 15 min, which was less than those observed with silicon dioxide (3.6 μm) and silicon dioxide (20 μm), even though they have equivalent specific surface area. As discussed earlier, when larger particles display specific surface area equivalent to smaller ones, it implies that the increment in surface area was the result of an increase in the number and length of pores. Therefore, the effect of particle size on drug release was similar to those observed with magnesium aluminum silicate (80 μm) discussed above.

Presence of the lipid formulation on the external surface of calcium silicate (25 μm [Hubersorb 5121[®]], Fig. 8C), as opposed to its retention within the pores of the adsorbent (Fig. 8A and B), had negative effect on griseofulvin release. Calcium silicate (25 μm [Hubersorb 5121[®]]) had the lowest surface area (Table 1) and was the only adsorbent that existed in agglomerated form at G-SEDDS to adsorbent ratio of 1:1. Presence of G-SEDDS on the surface of the adsorbent could be deduced from its flow behavior as shown in Fig. 3. The cumulative percent of griseofulvin released from this adsorbent after 60 min was 26.2% (Fig. 6) which was least among the adsorbents and was similar to the dissolution profile of micronized powder. Presence of a larger portion of the formulation in direct contact with the surface of calcium silicate (25 μm [Hubersorb 5121[®]]) increases the contact area (φ) between griseofulvin and the adsorbent. This leads to griseofulvin precipitation from the G-SEDDS due to hydrophobic interactions between the drug and the surface of the adsorbent.

To study the effect of formulation to adsorbent ratio on drug release, G-SEDDS was loaded on silicon dioxide (3.6 μm [GL100[®]]) at three different ratios and subjected to a dissolution study. The quantity of each blend was adjusted so that an equal amount of griseofulvin was used in the study. From the dissolution data, it was found that the cumulative percent of griseofulvin released from the adsorbent increased as the ratio of G-SEDDS to silicon dioxide increased from 0.5:1 to 1:1 to 1.5:1 (Fig. 7). Increasing the proportion of G-SEDDS in the blend shifted the dissolution profiles towards higher percentage release. As seen after 15 min, griseofulvin release increased from 16.0% to 28.2% to 43.7% as G-SEDDS to silicon dioxide increased from 0.5:1 to 1.5:1. Unlike calcium silicate (25 μm [Hubersorb 5121[®]]), G-SEDDS was retained within the pores of silicon dioxide (3.6 μm [GL100[®]]) at maximum loading ratio of 1.5:1. The retention of G-SEDDS within the pores is corroborated by the powder rheometry data presented in Fig. 2, which shows that the adsorbent was free flowing at the G-SEDDS to powder ratios used in this study. Therefore, while the decrease in griseofulvin release from calcium silicate (25 μm [Hubersorb 5121[®]]) was attributed to surface adsorption, the enhancement in griseofulvin release from silicon dioxide (3.6 μm [GL100[®]]) with increased G-SEDDS loading is ascribed to differences in the level of pore filling and presence of G-SEDDS as entrained droplets with minimal contact area within the perimeters of the pores. This finding strongly supports the notion that contact area confers a negative impact on griseofulvin release as depicted in Fig. 8.

4. Conclusion

SEDDS formulation could be readily adsorbed on silica and silicates. Changes in flow behavior as a function of SEDDS addition could be monitored using powder flow analyzer. It was found that the effect of SEDDS on the flow behavior of the adsorbent is similar to that observed in wet granulation process. Adsorption of

SEDDS, however, exhibits a lag or critical phase during which no change in flow is observed. This phase is attributed to the porous nature of silica and silicate adsorbents. During this phase, the SEDDS formulation is embedded within the carrier and entrapped in the intraparticle pores. Therefore, the duration of the lag phase depends on the adsorbing capacity, size, and specific surface area of the adsorbent. This phase could be used as a guide in formulation development to determine the extent of SEDDS addition without impacting flow. In addition, it could be used as a measure of the critical point after which further SEDDS addition would cause particle agglomeration. Furthermore, dissolution and release of the SEDDS from the adsorbent was found to be dependent on two key factors, the physical retention of the formulation in the pores and the area of contact between the formulation and the adsorbent. Both factors are dependent on the specific surface area and particle size of the adsorbent. Increase in the area of contact between the formulation and the surface of the adsorbent enhances the potential for nucleation, which decreases the extent of drug release. For similar-sized particles, formulation adsorbed on the surface of less porous particle such as calcium silicate (25 μm , Hubersorb 5121[®]) results in larger area of contact whereas its' entrainment as droplets in the pores of the more porous adsorbent reduces the area of contact for nucleation. Therefore, the overall area of contact between the lipid and the adsorbent is higher in the case of Hubersorb 5121[®] than in more porous material. Also, increase in particle size, while maintaining constant overall surface area, results in lengthier pores. This causes physical entrapment of the SEDDS in the pores and subsequently lower dissolution rates.

Acknowledgments

The authors would like to thank Bill Fultz, Nolan Phillips, and Dev K. Mehra (J. M. Huber Corp.) for their fruitful discussion.

References

- Amidon, G.E., 1995. Physical and mechanical property characterization of powders. In: Brittain, H.G. (Ed.), *Physical Characterization of Pharmaceutical Solids*. Marcel Dekker, New York, pp. 293–294.
- Brown, K.D., 2005. *Genet. Eng. Biotechnol. News* 25.
- Carr, R.L., 1965. Evaluating flow properties of solids. *Chem. Eng.* 18, 163–168.
- Cannon, J.B., 2005. Oral solid dosage forms of lipid-based drug delivery systems. *Am. Pharmaceut. Rev.* 8, 108–115.
- Chang, R.K., Raghavan, K.S., Hussain, M.A., 1998. A study on gelatin capsule brittleness: moisture transfer between the capsule shell and its content. *J. Pharm. Sci.* 87, 556–558.
- Chatlapalli, R.R., Bhagwan, D., 1998. Rheological characterization of diltiazem HCl/cellulose wet masses using a mixer torque rheometer. *Int. J. Pharm.* 175, 47–59.
- Craig, D.Q.M., Lievens, H.S.R., Pitt, K.G., Storey, D.E., 1993. An investigation into the physico-chemical properties of self-emulsifying systems using low frequency dielectric spectroscopy, surface tension measurements and particle size analysis. *Int. J. Pharm.* 96, 147–155.
- DeHaan, P., Poel-Janssen, H.G.M., 2001. Solid pharmaceutical composition comprising an excipient capable of binding water. United States Patent No. 6,187,339.
- Freeman, R.E., 2004. Predicting flowability and characterizing powders. *Pharm. Technol. Eur.* 16, 41–43.
- Goldszal, A., Bousquet, J., 2001. Wet agglomeration of powders: from physics towards process optimization. *Powder Technol.* 117, 221–231.
- Greiner, R.W., Evans, D.F., 1990. Spontaneous formation of a water-continuous emulsion from water-in oil microemulsion. *Langmuir* 6, 1793–1796.
- Gupta, M.K., Tseng, Y.C., Goldman, D., Bogner, R.H., 2002. Hydrogen bonding with adsorbent during storage governs drug dissolution from solid dispersion. *Pharm. Res.* 19, 1663–1672.
- Hariharan, M., Mehdizadeh, E., 2002. The use of mixer torque rheometry to study the effect of formulation variables on the properties of wet granulations. *Drug Dev. Ind. Pharm.* 28, 253–263.
- Hauss, D.J., Fogal, S.E., Ficorilli, J.V., Price, C.A., Roy, T., Jayaraj, A.A., Keirns, J.J., 1998. Lipid-based delivery systems for improving the bioavailability and lymphatic transport of a poorly water-soluble LT4 inhibitor. *J. Pharm. Sci.* 87, 164–169.
- Hodes, G., 2002. *Chemical Solution Deposition of Semiconductor Films*. Marcel Dekker Inc, pp. 12–24.
- Jannin, V., Chambin, O., 2005. Self emulsifying drug delivery systems. *STP Pharma Pratiques* 15, 247–254.
- Khoo, S.M., Humberstone, A.J., Porter, C.J.H., Edwards, G.A., Charman, W.N., 1998. Formulation design and bioavailability assessment of lipidic self-emulsifying formulations of halofantrine. *Int. J. Pharm.* 167, 155–164.
- Klauser, R.M., Irschik, H., Kletzmays, J., Sturm, L., Brunner, W., Woloszczuk, W., Kovarik, J., 1997. Pharmacokinetic cyclosporine A profile under long-term Neoral treatment in renal transplant recipients: does fat intake still matter? *Transplant Proc.* 29, 3137–3140.
- Kommuru, T.R., Gurley, B., Khan, M.A., Reddy, I.K., 2001. Self-emulsifying drug delivery systems (SEDDS) of coenzyme Q10: formulation development and bioavailability assessment. *Int. J. Pharm.* 212, 233–246.
- Liao, C., Jarowski, C.I., 1984. Dissolution rates of corticoid solutions dispersed on silicas. *J. Pharm. Sci.* 73, 401–403.
- Luukkonen, P., Schaefer, T., Podczek, F., Newton, M., Hellen, L., Yliiruusi, J., 2001. Characterization of microcrystalline cellulose wet masses using a powder rheometer. *Eur. J. Pharm. Sci.* 13, 143–149.
- MacGregor, K.J., Embleton, J.K., 1997. Influence of lipolysis on drug absorption from the gastrointestinal tract. *Adv. Drug Deliv. Rev.* 25, 33–46.
- Mei, X., Etzler, F.M., Wang, Z., 2006. Use of texture analyzer to study hydrophilic solvent effects on the mechanical properties of hard gelatin capsules. *Int. J. Pharm.* 324, 128–135.
- Navaneethan, C.V., Missaghi, S., Fassihi, R., 2005. Application of powder rheometer to determine powder flow properties and lubrication efficiency of pharmaceutical particulate systems. *AAPS PharmSciTech* 6, 49.
- Nazzal, S., Wang, Y., 2001. Characterization of soft gelatin capsules by thermal analysis. *Int. J. Pharm.* 230, 35–45.
- Nazzal, S., Nutan, M.P.A., Shah, R., Zaghoul, A.A., Khan, M.A., 2002a. Optimization of a self-nanoemulsified tablet dosage form of ubiquinone using response surface methodology: effect of formulation ingredients. *Int. J. Pharm.* 240, 103–114.
- Nazzal, S., Zaghoul, A.A., Khan, M.A., 2002b. Effects of extragranular microcrystalline cellulose on compaction, surface roughness, and in-vitro dissolution of a self-nanoemulsified solid dosage form of ubiquinone. *Pharm. Technol.* 26, 86–98.
- Pather, S.I., Gupte, S.V., Khankari, K., Hontz, J., Robinson, J.R., Eichman, J.D., Kumbale, R., 2001. Microemulsions as solid dosage forms for oral administration. U.S. Patent 6,280,770 B1 (issued August 28, 2001).
- Pather, S.I., Gupte, S.V., Khankari, K., Hontz, J., Kumbale, R., 2004. Emulsions as solid dosage forms for oral administration. U.S. Patent 6,692,771 B2 (issued February 17, 2004).
- Patil, P., Paradkar, A., 2006. Porous polystyrene beads as carriers for self-emulsifying system containing loratadine. *AAPS PharmSciTech* 7, 28.
- Podczek, F., 1999. Rheological studies of the physical properties of powders used in capsule filling. *Pharm. Technol. Eur.* 11, 16–24.
- Podczek, F., Newton, J.M., 2000. Powder and capsule filling properties of lubricated granulated cellulose powder. *Eur. J. Pharm. Biopharm.* 50, 373–377.
- Pouton, C.W., 2000. Lipid formulation for oral administration of drugs: non-emulsifying, self-emulsifying and 'self microemulsifying' drug delivery systems. *Eur. J. Pharm. Sci.*, S93–S98.
- Salonen, J., Laitinen, L., Kaukonen, A.M., Tuura, J., Björkqvist, M., Heikkilä, T., Vähä-Heikkilä, K., Hirvonen, J., Lehto, V.P., 2005. Mesoporous silicon microparticles for oral drug delivery: loading and release of five model drugs. *J. Control. Release* 108, 362–374.
- Spireas, S.S., Jarowski, C.I., Rohera, B.D., 1992. Powdered solution technology: principle and mechanism. *Pharm. Res.* 9, 1351–1358.
- Spireas, S., Sadu, S., Grover, R., 1998. In-vitro release evaluation of hydrocortisone liquisolid tablet. *J. Pharm. Sci.* 87, 867–872.
- Spireas, S., Sadu, S., 1998. Enhancement of prednisolone dissolution properties using liquisolid compacts. *Int. J. Pharm.* 166, 177–188.
- Thalberg, K., Lindholm, D., Axelsson, A., 2004. Comparison of different flowability tests for powders for inhalation. *Powder Technol.* 146, 206–213.
- Vyas, S.P., Jain, C.P., Kaushik, A., Dixit, V.K., 1992. Preparation and characterization of griseofulvin dry emulsion. *Pharmazie* 47, H.6.
- Yang, K.Y., Glemza, R.J., 1979. Effect of amorphous silicon dioxide on drug dissolution. *J. Pharm. Sci.* 68, 560–565.